Experimental report

28/08/2017

Proposal: 5-24-585 **Council:** 4/2016

Title: High Temperature investigation: crystal structure and phase stabilityof high thermoelectric performancephases: Cu8(Fe, Zn)3Sn2S12, Cu5FeS4

Research area: Materials

This proposal is a new proposal

Main proposer: **Emmanuel GUILMEAU**

Experimental team: Pavankumar VENTRAPATI
Emmanuel GUILMEAU
Pierric LEMOINE

Local contacts: Vivian NASSIF

Samples: Cu8Fe3Sn2S12
Cu5FeS4
CuMGeS (M=Mo, Fe,W)
CuVSnS
CuSnS
BiCuOS
NiNbP
CsMoBr

Instrument	Requested days	Allocated days	From	To
D1B	4	3	13/09/2016	16/09/2016

Abstract:

Following the discovery of a promising thermoelectric (TE) material: tetrahedrite - Cu10.5Ni1.5Sb4S13 various studies were carried out in order to reveal the beneficial role of Ni on the TE properties, purity and phase stability using NPD1. Recent investigations have shown that stannoidite compounds (Cu8(Fe, Zn)3Sn2S12) exhibits similar TE properties. However, the origins of these electrical properties together with the low thermal conductivity are still unclear. Numerous assumptions have correlated those properties to mixing in the valence of Cu and Fe or by a rattling effect induced by the Cu atoms. Unfortunately, our lab equipment does not allow confirming or rebutting these hypotheses. In parallel, we have also shown that the bornite compound (Cu5FeS4) also exhibits very low intrinsic thermal conductivity related to its complex (modulated) structure. This latter compound evidences two structural transitions at 473 K and 543 K; resulting in drastic modifications of the TE properties. In order to determine accurately the thermal evolution of both crystal structure and to provide a better understanding of the associated electrical properties, we need HT in situ NPD data.

Experimental report on the proposal 5-24-585: *High temperature investigation: crystal structure and phase stability of high thermoelectric performance phases: $Cu_8(Fe,Zn)_3Sn_2S_{12}$, Cu_5FeS_4.*

E. Guilmeau[1], V. Pavan Kumar[1], P. Lemoine[2], T. Barbier[1], V. Nassif[3]

[1] Laboratoire CRISMAT, UMR-CNRS 6508, ENSICAEN, 6 bd du maréchal Juin, 14050 Caen Cedex 4, France
[2] Institut des Sciences Chimiques de Rennes, UMR-CNRS 6226, 263 av du général Leclerc, CS 74205, 35042 Rennes, France
[3] Institut Néel, UPR-CNRS/UGA 2940, 25 rue des Martyrs, BP 166, 38042 Grenoble Cedex 9, France

1. Introduction

Recently, copper-containing ternary sulphides have enticed much attention for thermoelectric (TE) applications due to their high figure of merit $ZT = S^2T/\rho\kappa$ values associated with the higher earth abundancy, and lower cost and toxicity of their elements compared to metal tellurides such as PbTe, Bi_2Te_3 and $AgSbTe_2$. From the viewpoint of thermoelectricity, two classes of copper-based sulfides $Cu_xM_yS_z$ can be distinguished, exhibiting n-type and p-type conductivities, respectively. The n-type class is obtained for lower copper content materials (Cu/M ratio ≤ 1) as chalcopyrite $CuFeS_2$-type sulfides such as $CuFe_{1-x}In_xS_2$ [1] and $Cu_{1-x}Zn_xFeS_2$ [2], cubic isocubanite $CuFe_2S_3$ [3], and $Cu_4Sn_7S_{16}$ [4,5]. The p-type class of copper-based sulfides covers a broad range of compositions, from Cu/M ratio equal or close to 1 as in stannites Cu_2ZnXS_4 (X = Sn, Ge) [6,7], to copper-rich sulfides, with Cu/M ratios > 1 as in Cu_2SnS_3 [8] and in derivatives of stannoidite $Cu_8Fe_3Sn_2S_{12}$ [9], tetrahedrite $Cu_{12}Sb_4S_{13}$ [10-12], colusite $Cu_{26}V_2Sn_6S_{32}$ [13-15], and bornite Cu_5FeS_4 [16-18].

A common feature of these TE phases is their intrinsically low thermal conductivities κ originating from high structural complexities. Hence, a perfect knowledge of the crystal structure is necessary to explain the high TE properties of these materials. In complement to X-rays diffraction and transmission electron microscopy, neutron powder diffraction is a useful technique to determine accurately the crystal structure and the phase stability at high temperature of these TE materials.

2. Bornite Cu_5FeS_4 and $Cu_5FeS_{3.6}Se_{0.4}$

2.1. Structural details

The thermal analysis of the structural behavior of Cu_5FeS_4 and $Cu_5FeS_{3.6}Se_{0.4}$ has been characterized by high temperature *in situ* neutron powder diffraction. The analysis of the experimental data requires to take into consideration that the bornite exhibits three structural forms [19-22], depending on the temperature: the high temperature disordered cubic form *C* (*Fm-3m*, $a_C \sim 5.50$ Å), the intermediate semi-ordered intermediate cubic form *IC* (*Fm-3m*, $a_{IC} \sim 2a_C$) and the ordered orthorhombic form *O* (*Pbca*, $a_O \sim 10.95$ Å, $b_O \sim 21.86$ Å, $c_O \sim 10.95$ Å). The high temperature cubic form exhibits a metal-deficient anti-fluorite type of structure (Fig. 1a) with iron, copper and cationic vacancies distributed at random in the tetrahedral sites formed by the cubic face centered framework of sulfide ions according to the formulation $[Cu_5Fe\square_2]S_4$, where □ represents vacancy. The two other forms, intermediate cubic and orthorhombic, correspond to a complex ordering of the transition elements and cationic vacancies and can in fact be considered as superstructures of the high temperature form. Their structures can be described as the combination of two cubic sub-cells. In one of these cubic sub-cells, formulated as $[Cu_6Fe_2]S_4$ the tetrahedral sites are fully occupied at random by copper and iron (Fig. 1b).

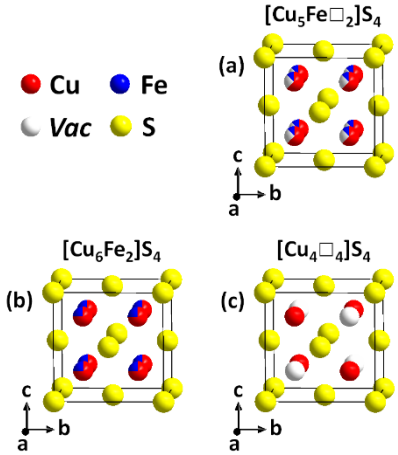

Fig. 1: Schematic representation of the basic unit sub-cells of three polymorphs of bornite: (a) $[Cu_5Fe\square_2]S_4$; statistical distribution of copper (red), iron (blue) and vacancies (white), (b) $[Cu_6Fe_2]S_4$; where copper and iron are randomly distributed, and (c) $[Cu_4\square_4]S_4$; ordered arrangement of copper and vacancies [18].

In the second sub-cell, the S_4 tetrahedra are half occupied by copper and the latter are distributed in an ordered way with cationic vacancies according to the formula $[Cu_4\square_4]S_4$ (Fig. 1c). As a consequence the two forms, orthorhombic and intermediate cubic, are built up of similar $[Cu_6Fe_2]S_4$ and $[Cu_4\square_4]S_4$ sub-cells and only differ by the ordered distribution of these sub-cells (Fig. 2). The three structures are very closely related, the *IC* form being a superstructure of the *C* form, and the structural transitions are topotactic [20].

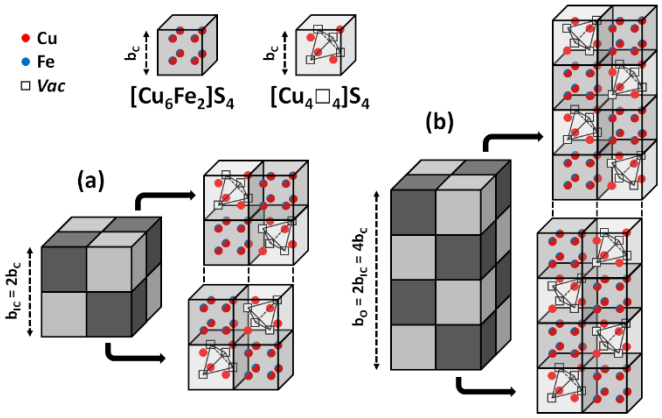

Fig. 2: Distribution of the cubic $[Cu_6Fe_2]S_4$ and $[Cu_4\square_4]S_4$ sub-cells in (a) the intermediate cubic and (b) orthorhombic ordered forms of bornite [18].

2.2. High temperature neutron powder diffraction

High temperature NPD data collected on pristine Cu_5FeS_4 from room temperature up to 673 K (Fig. 3a) show that SPS process enables the stabilization of the intermediate cubic (IC) semi-ordered form at the expense of the ordered orthorhombic (O) form in the 300-475 K temperature range. It also highlights that the intensities of the superstructure reflections corresponding to the *O* form increases with the temperature up to ~ 460 K, indicating an improvement of the crystallinity of the phase with the temperature, especially in the range 420-460 K (Fig.3b and c). At higher temperature NPD data show that the intensity of the diffraction peaks of the *O* form decreases rapidly above 460 K at the benefit of the *IC* (+*C*) forms and that above 580 K, the *IC* form is totally transformed into the *C* form (Fig. 3d and e) and other phases related to the chalcopyrite-type $CuFeS_2$ (Fig. 3a).

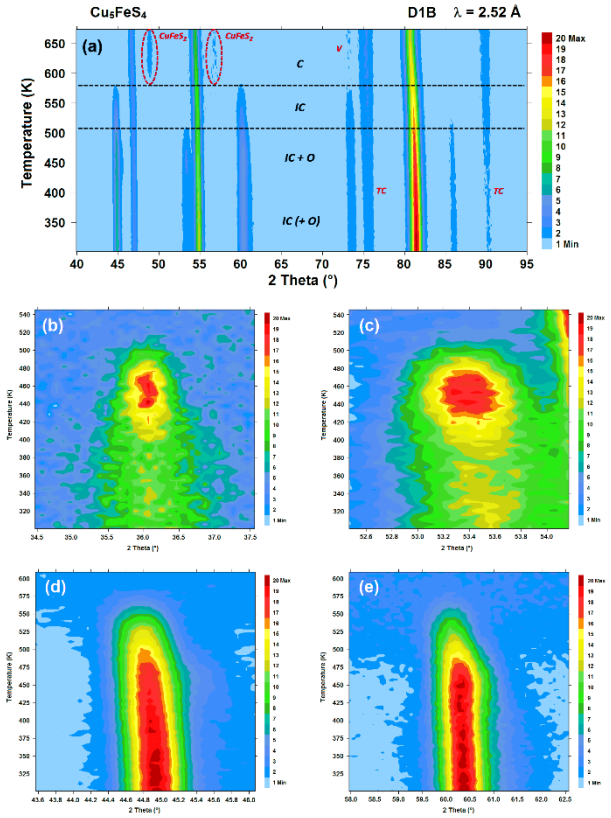

Fig. 3: 2D-plots of (a) neutron powder thermo-diffractogram, and (b to e) thermal evolution of some characteristic diffraction peaks of Cu_5FeS_4 recorded between 300 K and 673 K (λ = 2.52 Å). The diffraction peaks of vanadium sample holder and thermocouple are labelled as V and TC, respectively.

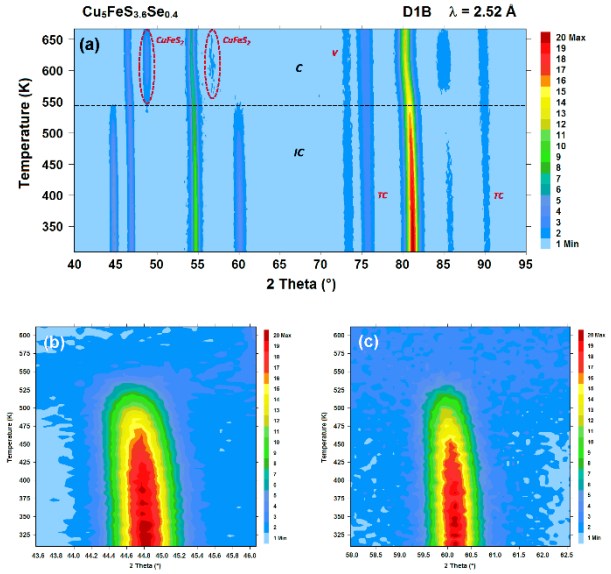

Fig. 4: 2D-plots of (a) neutron powder thermo-diffractogram, and (b and c) thermal evolution of some characteristic diffraction peaks of $Cu_5FeS_{3.6}Se_{0.4}$ recorded between 300 K and 673 K (λ = 2.52 Å). The diffraction peaks of vanadium sample holder and thermocouple are labelled as V and TC, respectively.

The neutron powder thermodiffractograms of the $Cu_5FeS_{3.6}Se_{0.4}$ sample recorded from 300 K to 673 K (Fig. 4a) highlights some significant differences compared to the data recorded from the pristine sample. In the low temperature range, *i.e.* $300 \leq T/K \leq 540$ K, only the diffraction peaks of the *IC* (+*C*) forms are observed. In contrast to the pristine compound, the diffraction peaks typical of the orthorhombic form are not detectable by increasing the temperature. It confirms that the Se for S substitution plays a crucial role in the structural stability of the cubic forms at low temperatures. The *IC* form is stable from RT to about 475 K (Fig. 4b and c), indicating that the cubic phase probably starts to be formed from this temperature. Beyond 540 K, the high temperature cubic form coexists with other phases related to the chalcopyrite-type structure (Fig. 4a).

Thus, the results highlight that, in both Cu_5FeS_4 and $Cu_5FeS_{3.6}Se_{0.4}$ compounds, the *IC* (+*C*) form is stabilized at lower temperature with respect to the ordered orthorhombic phase due to the specific SPS sintering conditions. Moreover, they clearly show that the structural transition from *IC* to *C* starts for both compounds at about 475 K, and is extended up to ~580 K and ~540 K for Cu_5FeS_4 and $Cu_5FeS_{3.6}Se_{0.4}$, respectively. These results are already published in Dalton Transactions [18].

3. Stannoidite $Cu_8(Fe,Zn)_3Sn_2S_{12}$

Neutron diffraction patterns of stannoidite $Cu_8(Fe,Zn)_3Sn_2S_{12}$ samples were recorded at room temperature, but for a full characterization of the complex crystal structure of these materials extra high resolution NPD measurements are needed. It will be done in the next few months on D2B thanks to the accepted proposal 5-21-1112.

4. References

[1] H. Xie, X. Su, G. Zheng, Y. Yan, W. Liu, H. Tang, M.G. Kanatzidis, C. Uher, X. Tang, *J. Phys. Chem. C* 120 **2016** 27895.
[2] H. Xie, X. Su, G. Zheng, T. Zhu, K. Yin, Y. Yan, C. Uher, M.G. Kanatzidis, X. Tang, *Adv. Energy, Mater.* 7 **2017** 1601299.
[3] T. Barbier, D. Berthebaud, R. Frésard, O.I. Lebedev, E. Guilmeau, V. Eyert, A. Maignan, *Inorg. Chem. Front.* 4 **2017** 424.
[4] J.P.F. Jemetio, P. Zhou, H. Kleinke, *J. Alloys Compd.* 417 **2006** 55.
[5] C. Bourgès, P. Lemoine, O.I. Lebedev, R. Daou, V. Hardy, B. Malaman, E. Guilmeau, *Acta Mater.* 97 **2015** 180.
[6] M.L. Liu, F.Q. Huang, L.D. Chen, I.W. Chen, *Appl. Phys. Lett.* 94 **2009** 202103.
[7] C.P. Heinrich, T.W. Day, W.G. Zeier, G.J. Snyder, W. Tremel, *J. Am. Chem. Soc.* 136 **2014** 442.
[8] Y. Shen, C. Li, R. Huang, R. Tian, Y. Ye, L. Pan, K. Koumoto, R. Zhang, C. Wan, Y. Wang, *Sci. Rep.* 6 **2016** 32501.
[9] V. Pavan Kumar, T. Barbier, V. Caignaert, B. Raveau, R. Daou, B. Malaman, G. Le Caër, P. Lemoine, E. Guilmeau, *J. Phys. Chem. C* 121 **2017** 16454.
[10] K. Suekuni, K. Tsuruta, T. Ariga, M. Koyano, *Appl. Phys. Express* 5 **2012** 51201.
[11] X. Lu, D.T. Morelli, Y. Xia, F. Zhou, V. Ozolins, H. Chi, X. Zhou, C. Uher, *Adv. Energy Mater.* 3 **2013** 342.
[12] T. Barbier, P. Lemoine, S. Gascoin, O.I. Lebedev, A. Kaltzoglou, P. Vaqueiro, A.V. Powell, R.I. Smith, E. Guilmeau, *J. Alloys Compd.* 634 **2015** 253.
[13] K. Suekuni, F.S. Kim, H. Nishiate, M. Ohta, H.I. Tanaka, T. Takabatake, *Appl. Phys. Lett.* 105 **2014** 132107.
[14] C. Bourgès, M. Gilmas, P. Lemoine, N.E. Mordvinova, O.I. Lebedev, E. Hug, V. Nassif, B. Malaman, R. Daou, E. Guilmeau, *J. Mater. Chem. C* 4 **2016** 7455.
[15] Y. Kikuchi, Y. Bouyrie, M. Ohta, K. Suekuni, M. Aihara, T. Takabatake, *J. Mater. Chem. A* 4 **2016** 15207.
[16] P. Qiu, T. Zhang, Y. Qiu, X. Shi, L. Chen, *Energy Environ. Sci.* 7 **2014** 4000.
[17] G. Guélou, A.V. Powell, P. Vaqueiro, *J. Mater. Chem. C* 3 **2015** 10624.
[18] V. Pavan Kumar, T. Barbier, P. Lemoine, B. Raveau, V. Nassif, E. Guilmeau, *Dalt. Trans.* 46 **2017** 2174.
[19] N. Morimoto, G. Kullerud, *Am. Mineral.* 46 **1961** 1270.
[20] A. Deschanvres, B. Raveau, *Rev. Chim. Miner.* 5 **1968** 221.
[21] K. Koto, N. Morimoto, *Acta Crystallogr., Sect. B: Struct. Crystallogr. Cryst. Chem.* 31 **1975** 2268.
[22] Y. Kanazawa, K. Koto, N. Morimoto, *Can. Mineral.* 16 **1978** 397.